

# Ruling the Control Authority of a Service Robot based on Information Precision

Valerio Magnago, Marco Andreetto, Stefano Divan, Daniele Fontanelli and Luigi Palopoli

**Abstract**—We consider the problem of guiding a senior user along a path using a robotic walking assistant. This is a particular type of path following problem, for which most of the solutions available in the literature require an exact localisation of the robot in the environment. An accurate localisation is obtained either with a heavy infrastructure (e.g., an active sensing system deployed in the environment or deploying landmarks in known positions) or using SLAM approaches with a massive data collection. Our key observation is that the intervention of the system (and a good level of accuracy) is only required in proximity of difficult decision points, while we can rely on the user in an environment where the only possibility is just to maintain a course (e.g., a corridor). The direct implication is that we can instrument the environment with a heavy infrastructure only in certain areas. This design strategy has to be complemented by an adequate control law that shifts the authority (i.e., the control of the actuators) between the robot and the user according to the accuracy of the information available to the robot. Such a control law is exactly the contribution of this paper.

## I. INTRODUCTION

Authority sharing is a new control paradigm in which the control action is decided by seeking a tradeoff between the control goals (e.g., staying on a course) and the decisions of a human who interacts with the system (e.g., the driver of a car). The exact balance between user and controller can change according to the circumstances. The approach is increasingly popular [1], [2] and its potential application areas are very many. One of the most promising is for robots providing assistance to older adults in their navigation of large and complex spaces. The importance and the potential market opportunities of this type of system stays in the recognised benefit of prolonging autonomous life through a sustained level of physical activity [3], [4]. In the ACANTO project [5], a commercial walker has been turned into an assistive robotics system called *FriWalk*. This service robot has cognitive abilities to plan a safe path satisfying the user requirements [6], to localise itself in the environment [7], [8], to plan deviation from the course in case of unforeseen obstacles [9], and to guide the user along the planned path using a number of mechanical guidance algorithms [2], [10],

[11], [12]. Mechanical guidance for assistive robots can be seen as a path following problem of a peculiar kind.

The solution to the path following problem is typically designed by supposing that the localisation algorithm is “accurate enough” to produce a negligible error in the estimate of the vehicle state [13]. Assuming a good localisation accuracy is fairly acceptable for robots relying on exogenous sensor readings (absolute measures) always or most of the times. Indeed, endogenous sensors (relative measures) are affected by the well known dead-reckoning effect that produces an unbounded growth of the position uncertainty [14], [15]. Several ways have been proposed to improve the accuracy of the robot localisation in the environment. Some authors propose an optimal deployment of landmarks [16] to meet a desired target accuracy [17], [18], [19]. Other authors propose using placing active sensors [20], [21], [22] or mapping the environment to detect landmarks [23], [24]. Whatever the strategy used to deploy and use markers in the environment, a certain fact with this type of solution is that the absolute position measures come intermittently. It is well known [25], [7] that closing a control loop with intermittent observation can lead to a poor performance (possibly even to instability) if the average rate is not sufficient to compensate for the system dynamics. On the other hand a massive deployment of landmarks is inconceivable in realistic environments (e.g., a museum, or a shopping mall). Authority sharing offers an elegant and unexpected escape from this quandary. The key observation is that even a user with mild cognitive impairments is able to maintain a direction of motion when the environment does not require choices (e.g., a corridor). Only in presence of decision points (e.g., bifurcations, cross-roads, doors) is a constant intervention of the system required. A possible way to see this is that the intelligence of the user can be used to compensate the reduced information precision on the environment. This behaviour mimics what usually happens in real life. A human being driving his/her car will override the suggestions coming from the navigator if the GPS localisation is evidently wrong or if an unforeseen obstacle, i.e. road works, blocks the suggested way. Similarly, the autonomous driving system of modern cars gives back the control to the human in case, e.g., of heavy weather [26].

We can translate the simple idea outlined above into a design principle: use a heavy infrastructure (dense landmarks) when a close support is required for the user and a light infrastructure (i.e., sparse landmarks) when we can shift the authority to the user. This natural strategy has to be complemented by a control algorithm that decides the

This project has received funding from the European Unions Horizon 2020 Research and Innovation Programme - Societal Challenge 1 (DG CON-NECT/H) under grant agreement n° 643644 “ACANTO - A CyberphysicsAI social NeTwOrk using robot friends”.

D. Fontanelli is with the Department of Industrial Engineering (DII), University of Trento, Via Sommarive 5, Trento, Italy [daniele.fontanelli@unitn.it](mailto:daniele.fontanelli@unitn.it). V. Magnago, M. Andreetto, S. Divan and L. Palopoli are with the Department of Information Engineering and Computer Science (DISI), University of Trento, Via Sommarive 5, Trento, Italy {[marco.andreetto](mailto:marco.andreetto), [stefano.divan](mailto:stefano.divan), [valerio.magnago](mailto:valerio.magnago), [luigi.palopoli](mailto:luigi.palopoli)}@unitn.it

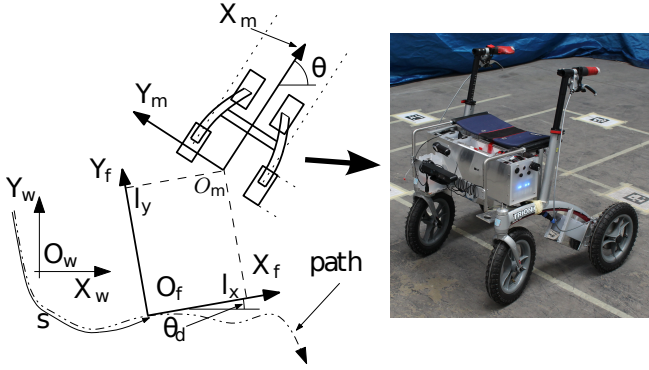


Fig. 1. Reference frames and corresponding vehicle coordinates.

balance of the authority according to the accuracy of the information on the system state, which is the most important contribution of the paper. Specifically, we propose a hybrid control scheme with two states: robot in control and human in control. The control scheme is Lyapunov based and gives the authority to one of the two states according to the available localisation precision or when the deviation from the path becomes relevant. The performance on the path following maximum error are experimentally characterised as a function of the uncertainty growth due to dead-reckoning. This could allow us to offer performance guarantees for known hardware and the environment are known.

The paper is organised as follows. Section II presents the mathematical background, formalises the path following problem and gives an overview of the solution exploiting a Lyapunov function. Section III presents a deep mathematical analysis of the probabilistic authority-sharing adopted control law. Section IV reports simulations performed to understand the overall behaviour of the solution, meanwhile, section V, deeply analyses experiments in a real environment. To conclude, section VI ends the paper with some final remarks.

## II. PROBLEM DEFINITION AND BACKGROUND MATERIAL

The *FriWalk* is modelled as a unicycle-like vehicle, as depicted in Figure 1. Let  $(x, y)$  be the coordinates of the mid point of the rear axle in a world reference frame  $\langle W \rangle = \{O_w, X_w, Y_w, Z_w\}$  and  $\theta$  the vehicle yaw, i.e. the orientation of the vehicle-attached reference frame  $\langle M \rangle = \{O_m, X_m, Y_m, Z_m\}$  with respect to the world frame (see Figure 1). The differential kinematic model with respect to the state variables  $\chi^* = [x, y, \theta]^T$  is given by

$$\begin{cases} \dot{x} = v \cos \theta, \\ \dot{y} = v \sin \theta, \\ \dot{\theta} = \omega, \end{cases} \quad (1)$$

where  $v$  and  $\omega$  are the forward and the angular velocity of the vehicle, respectively. In passive robotics, the forward velocity is typically selected or imposed by the user. The angular velocity is considered as a control input, and it is applied using actuation systems such as front steering wheels [10], brakes [2], [12] or rear motors [11]. The path

following problem is described by adopting a Frenet frame  $\langle F \rangle = \{O_f, X_f, Y_f, Z_f\}$  moving along the path and defining the curvilinear abscissa  $s$  (see Figure 1). The orientation of the Frenet frame (i.e. the desired attitude of the vehicle) is denoted by  $\theta_d$ , while the vehicle reference point  $O_m$  has coordinates  $(l_x, l_y)$  in the Frenet frame  $\langle F \rangle$ . The orientation error is thus defined as  $\tilde{\theta} = \theta - \theta_d$ . Using this new set of coordinates  $[l_x, l_y, \tilde{\theta}]$ , the rollator differential kinematics (1) is rewritten as [27]

$$\begin{cases} \dot{l}_x = -\dot{s}(1 - c(s)l_y) + v \cos \tilde{\theta}, \\ \dot{l}_y = -c(s)\dot{s}l_x + v \sin \tilde{\theta}, \\ \dot{\tilde{\theta}} = \omega - c(s)\dot{s}, \end{cases} \quad (2)$$

where the path curvature is  $c(s) = \frac{d\theta_d}{ds}$ , and the velocity of the Frenet frame origin  $\dot{s}$  is an auxiliary control input that can be freely chosen. The coordinates  $\chi = [l_x, l_y, \tilde{\theta}]^T$  are used to represent the path following problem as an asymptotic stability problem. The path is indeed approached and followed if

$$\lim_{t \rightarrow +\infty} |l_x(t)| = \lim_{t \rightarrow +\infty} |l_y(t)| = \lim_{t \rightarrow +\infty} |\tilde{\theta}(t)| = 0, \quad (3)$$

where  $t$  is the time.

### A. Path following

The solution to the path following problem is typically designed by supposing that the localisation algorithm is “accurate enough” to yield a negligible error on the estimate of the vehicle state  $\chi$ . Of course, when intermittent observations are adopted, as in the localisation system running on the *FriWalk* and reported in [7], the effect of the feedback control can be highly wrong and, hence, the control should be given to the user. To implement this authority-sharing, how the localisation accuracy is derived and a description of the controller implemented is needed, which is the purpose of this section.

1) *Vehicle localisation*: Let us denote  $\hat{a}$  the estimate of the quantity  $a$  and  $\sigma_a$  the corresponding standard deviation. With localisation algorithm we intend the execution of an estimator that provides “suitable estimates” of  $\hat{x}, \hat{y}$  and  $\hat{\theta}$  of the vehicle states of (1). For the rollator in Figure 1, the available sensors are encoders mounted on the rear wheels (odometry-based localisation) and a camera reading landmarks (QR codes placed on the floor, the ceiling or on the walls) whose positions in the map are known. The odometry data are always available but affected by dead-reckoning. The measures of vehicle position and attitude obtained by the landmarks are absolute but available only when a landmark is in the field of view of the camera. The two measures are fused using a Bayesian estimator, such as an Extended Kalman filter [14]. The estimator returns minimum variance estimates  $\hat{x}, \hat{y}$  and  $\hat{\theta}$  of the vehicle state and the corresponding estimation error covariance matrix

$$P = E \left\{ [x - \hat{x}, y - \hat{y}, \theta - \hat{\theta}]^T [x - \hat{x}, y - \hat{y}, \theta - \hat{\theta}] \right\}, \quad (4)$$

where  $E\{\cdot\}$  is the expected value operator.

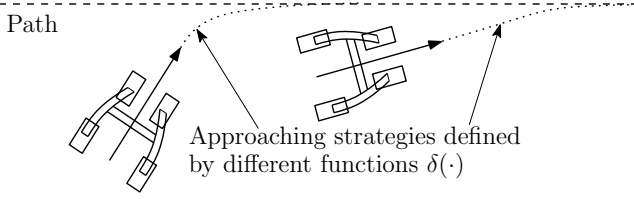


Fig. 2. Examples of approaching manoeuvres.

2) *Path following controller*: It is a common practice in path following problems, to introduce a steering angle  $\delta$  describing the manoeuvre that the vehicle should take to properly approach and follow the path, as sketched in Figure 2. For a vehicle moving forward (i.e.  $\lim_{t \rightarrow \infty} v(t) > 0$ ), if  $\delta(\cdot)$  is a continuous, strictly monotonic and odd function of  $l_y$  in (2) and satisfying  $l_y \delta(l_y) \leq 0$  and  $|\delta(l_y)| < \frac{\pi}{2}$ ,  $\forall l_y$ , and the velocity of the Frenet frame  $\langle F \rangle$  is computed as  $\dot{s} = v(\cos \tilde{\theta} + \kappa_x l_x)$ , where  $\kappa_x > 0$ , it is sufficient to design a control input  $\omega(\chi)$  that asymptotically drives to zero the attitude error  $e_\theta = \theta - \delta(l_y)$  to solve the path following problem (3) (see, for instance, [27]). A control law satisfying this requirement is

$$\begin{aligned} \omega(\chi) &= v \left[ \gamma(\chi) - \kappa \left( \tilde{\theta} - \delta(l_y) \right) \right], \\ \gamma(\chi) &= c(s)(\cos(\tilde{\theta}) + \kappa_x l_x) + \\ &\quad + \left[ -c(s)(\cos(\tilde{\theta}) + \kappa_x l_x) l_x + \sin(\tilde{\theta}) \right] \delta'(l_y), \end{aligned} \quad (5)$$

where  $\kappa > 0$  is a gain to be selected and  $\delta'(l_y) \triangleq \frac{d\delta}{dl_y}(l_y)$ . Indeed, using the Lyapunov function

$$V = \frac{1}{2} e_\theta^2, \quad (6)$$

its time derivative is

$$\begin{aligned} \dot{V} &= e_\theta \dot{e}_\theta = e_\theta \left( \omega - c(s)\dot{s} - \dot{l}_y \delta'(l_y) \right) = \\ &= e_\theta (\omega - v\gamma(\chi)) = -v\kappa e_\theta^2 < 0, \quad \forall e_\theta \neq 0, \end{aligned} \quad (7)$$

i.e.  $e_\theta = 0$  is a uniformly globally asymptotically stable equilibrium.

### III. PROBABILISTIC AUTHORITY-SHARING CONTROLLER

The controller (5) ensures asymptotic tracking of the path in ideal conditions (i.e. the estimation error of  $\chi$  is zero). Intuitively, if the estimation error is limited, controller (5) is expected to ensure that the path is followed with an error due to (7). However, if no landmark is detected, hence no absolute measure is available, the localisation is affected by dead-reckoning of odometry and hence the estimation error grows potentially unbounded. Hence, the path following error grows as well. In this following section we will show the guard adopted to shift the control authority between the robot and the user and how this authority-sharing idea can be formally model using tools from hybrid systems [28].

#### A. Controller probabilistic analysis

To explain the rationale of the probabilistic analysis of the controller, let us specify what changes in (7) when the state  $\chi$  is not known, the control input  $\omega(\cdot)$  in (5) is computed using the available estimate  $\hat{\chi}$ , which is affected by the estimation error noise  $\varepsilon$ , i.e.

$$\varepsilon = \begin{bmatrix} \varepsilon_x \\ \varepsilon_y \\ \varepsilon_\theta \end{bmatrix} = \begin{bmatrix} l_x - \hat{l}_x \\ l_y - \hat{l}_y \\ \tilde{\theta} - \hat{\theta} \end{bmatrix} = \chi - \hat{\chi}. \quad (8)$$

Using the Taylor expansion for the nonlinear functions in (5) about the estimated quantities, and recalling (8), one gets

$$\begin{aligned} \gamma(\chi) &= c(s)\Theta(\hat{\chi}, \varepsilon) + \left( \delta'(\hat{l}_y) + \delta''(\hat{l}_y)\varepsilon_y \right) \\ &\quad \left[ -c(s)\Theta(\hat{\chi}, \varepsilon)(\hat{l}_x + \varepsilon_x) + \sin(\hat{\theta}) + \cos(\hat{\theta})\varepsilon_\theta \right] + \mathcal{O}(\varepsilon^2), \end{aligned}$$

where  $\delta'(\hat{l}_y) = \frac{d\delta}{dl_y}(l_y) \Big|_{l_y=\hat{l}_y}$  and  $\delta''(\hat{l}_y) = \frac{d^2\delta}{dl_y^2}(l_y) \Big|_{l_y=\hat{l}_y}$ , where, with a light abuse of notation, we denote with  $\mathcal{O}(\varepsilon^2)$  high order error terms, and where

$$\Theta(\hat{\chi}, \varepsilon) = \cos(\hat{\theta}) - \sin(\hat{\theta})\varepsilon_\theta + \kappa_x \hat{l}_x + \kappa_x \varepsilon_x.$$

Hence

$$\gamma(\chi) = \gamma(\hat{\chi}) + H(\kappa_x, s, \hat{\chi})\varepsilon + \mathcal{O}(\varepsilon^2), \quad (9)$$

where  $H(\kappa_x, s, \hat{\chi})$  is a row vector equals to

$$\begin{bmatrix} c(s)\kappa_x - c(s)\delta'(\hat{l}_y) \left( \cos(\hat{\theta}) + 2\kappa_x \hat{l}_x \right) \\ \left[ -c(s) \left( \cos(\hat{\theta}) + \kappa_x + \hat{l}_x \right) \hat{l}_x + \sin(\hat{\theta}) \right] \delta''(\hat{l}_y) \\ c(s) \sin(\hat{\theta}) \left( \hat{l}_x \delta'(\hat{l}_y) - 1 \right) + \cos(\hat{\theta}) \delta'(\hat{l}_y) \end{bmatrix}^T.$$

We can therefore compute the first order approximation of (7) as

$$\dot{V} = e_\theta \dot{e}_\theta = e_\theta (\omega(\hat{\chi}) - v\gamma(\chi)) = e_\theta (v\gamma(\hat{\chi}) - \kappa v \hat{e}_\theta - v\gamma(\chi)),$$

and then, noticing that  $\hat{e}_\theta = \hat{\theta} - \delta(\hat{l}_y)$  and that

$$e_\theta = \hat{\theta} + \varepsilon_\theta - \left[ \delta(\hat{l}_y) + \delta'(\hat{l}_y)\varepsilon_y + \mathcal{O}(\varepsilon_y^2) \right] = \hat{e}_\theta + G(\hat{l}_y)\varepsilon + \mathcal{O}(\varepsilon_y^2),$$

where  $G(\hat{l}_y) = [0, -\delta'(\hat{l}_y), 1]$ , and then plugging (9), we finally have

$$\begin{aligned} \dot{V} &= e_\theta (v\gamma(\hat{\chi}) - \kappa v \hat{e}_\theta - v\gamma(\chi)) \\ &= \left( \hat{e}_\theta + G(\hat{l}_y)\varepsilon + \mathcal{O}(\varepsilon_y^2) \right) \\ &\quad (v\gamma(\hat{\chi}) - \kappa v \hat{e}_\theta - v\gamma(\hat{\chi}) - vH(\kappa_x, s, \hat{\chi})\varepsilon + \mathcal{O}(\varepsilon^2)) \\ &= -v\kappa \hat{e}_\theta^2 - v\hat{e}_\theta \left( \kappa G(\hat{l}_y) - H(\kappa_x, s, \hat{\chi}) \right) \varepsilon + \mathcal{O}(\varepsilon^2) \\ &= -v\kappa \hat{e}_\theta^2 - v\hat{e}_\theta \Xi(\kappa, \kappa_x, s, \hat{\chi})\varepsilon + \mathcal{O}(\varepsilon^2) \\ &= -v\kappa \hat{e}_\theta^2 + f(\varepsilon), \end{aligned} \quad (10)$$

where  $f(\cdot)$  is a nonlinear function of the estimation error. It is evident that the negative definiteness cannot be established. Moreover, if the noise affecting the measures is Gaussian,  $\varepsilon$  could be unbounded, which rules out standard

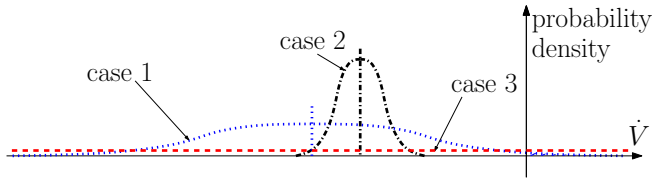


Fig. 3. Examples of distributions of Lyapunov function derivatives.

techniques, such as proving the boundedness of the Lyapunov function [29]. More importantly, even if a bound can be determined, it is not given for granted that the human using the *FriWalk* could not do anything better. Instead, notice that the Lyapunov function derivative  $\dot{V}$  in (10) is a random variable since it depends on  $\varepsilon$ .

**Definition 1 (Controller reliability):** Given  $\Gamma \leq 0$ , the reliability  $p_\Gamma(\hat{\chi})$  of a control action  $\omega(\hat{\chi})$  is given by probability

$$p_\Gamma(\hat{\chi}) = \Pr[\dot{V} < v\Gamma], \quad (11)$$

where  $\Pr[\dot{V} < v\Gamma]$  denotes the probability that the event  $\dot{V} < v\Gamma$  takes place.

The constant  $\Gamma \leq 0$  is a minimum convergence speed that the controller is required to guarantee. Roughly speaking, the reliability  $p_\Gamma(\hat{\chi})$  is the probability that the controller ensures at least such convergence speed. Scaling  $\Gamma$  by  $v$  is not strictly necessary but it comes handy since  $\dot{V}$  is linear with respect to  $v$  as well. In fact, if the controller were deterministic as in (7), we would get  $\dot{V} < v\Gamma \iff -v\kappa e_\theta^2 < v\Gamma \iff -\kappa e_\theta^2 < \Gamma$ .

Using (10), it is now possible to compute a first order approximation of the mean value  $\bar{\dot{V}}$  and of the standard deviation  $\sigma_{\dot{V}}$ , which are required to compute the controller reliability as per Definition 1. Assuming as customary that  $E\{\varepsilon\} = 0$ , we can readily have

$$\begin{aligned} \bar{\dot{V}} &= E\{\dot{V}\} = -v\kappa\hat{e}_\theta^2 \\ \sigma_{\dot{V}}^2 &= E\left\{\left(\dot{V} - E\{\dot{V}\}\right)^2\right\} \\ &= E\left\{v^2\hat{e}_\theta^2\Xi(\kappa, \kappa_x, s, \hat{\chi})\varepsilon\varepsilon^T\Xi(\kappa, \kappa_x, s, \hat{\chi})^T\right\} \\ &= v^2\hat{e}_\theta^2\Xi(\kappa, \kappa_x, s, \hat{\chi})P_\varepsilon\Xi(\kappa, \kappa_x, s, \hat{\chi})^T. \end{aligned} \quad (12)$$

By denoting with  $\chi = \Phi(\chi^*)$  the diffeomorphism between the two state spaces and with  $J_\Phi$  its Jacobian, we immediately have that  $P_\varepsilon = J_\Phi P J_\Phi^T$ , where  $P$  has been defined in (4) as the localisation algorithm estimator. Under the assumption of Gaussian distribution, using mean value and covariance from (12), the probability (11) can be explicitly computed.

The idea proposed in this paper is to allocate the control authority on the basis of the controller reliability (11). To intuitively describe this approach, we compare case 1 and case 2 in Figure 3. Suppose for simplicity that  $\Gamma = 0$  in the definition of controller reliability (11). The mean value of  $\dot{V}$  in case 1 is smaller (i.e. larger convergence rate) than case 2, while its covariance is much larger than the covariance of case 2. This implies that the reliability of the

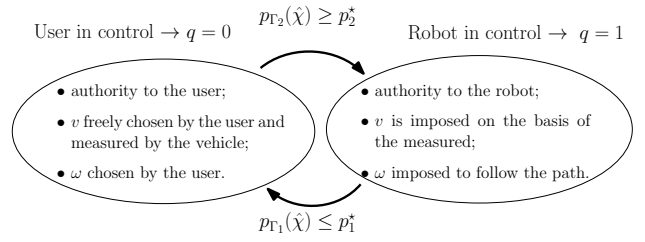


Fig. 4. Control authority sharing of the hybrid controller (14).

controller is larger in case 2, since the probability to get  $\dot{V} < 0$  is larger than case 1. Consider also case 3, where the covariance tends to infinity, i.e. absence of information. Since the controller reliability is in this case 0.5, any action the robot performs has 50% chance of reducing the attitude error  $e_\theta$ .

**Remark 1:** When  $e_\theta \rightarrow 0$ , the controller reliability decreases (see (11)), hence a higher probability of having the human in control of the vehicle is of course expected. By noting that  $\dot{V}$  is a quadratic function of  $e_\theta$ , those points correspond also to the region in which the first order linear approximation in (12) is less reliable. By combining this observation with the fact that in those points the control effort is also smaller, a certain degree of robustness of the proposed approach to linearisation errors can also be inferred.

### B. Hybrid authority-sharing

The control authority is shared with the user on the basis of the controller reliability, as shown in Figure 4. To properly implement a smooth transition, we define an hysteresis mechanism by formulating the control law as a hybrid system [28]. More in depth, let  $q \in \{0, 1\}$  be a logic variable defining who retains the control authority. If  $q = 0$  the controller reliability is small and then the user is in control of the vehicle, i.e. the vehicle actuators are not active (*user in control* state in Figure 4). While if  $q = 1$  the controller reliability is large and hence the robot is in control (*robot in control* state in Figure 4 and the control action (5) is applied to steer the vehicle towards the path). The hysteresis is defined on the basis of two constants  $\Gamma_2 > \Gamma_1 \geq 0$  representing convergence speed thresholds. Let  $p_1^* \in (0, 1)$  and  $p_2^* \in (0, 1)$ ,  $p_1^* \leq p_2^*$ , be the minimum tolerated reliabilities that, respectively, activate and disengage the controller. The overall controller is formalised as the following hybrid system having state  $[e_\theta, q]^T$ .

$$\begin{cases} \dot{q} &= 0, & [e_\theta, q]^T \in \mathcal{C}, \\ q^+ &= 1 - q, & [e_\theta, q]^T \in \mathcal{D}, \end{cases} \quad (13)$$

where  $\mathcal{C} := \mathcal{C}_0 \cup \mathcal{C}_1$  and  $\mathcal{D} := \mathcal{D}_0 \cup \mathcal{D}_1$  are the flow and the jump set respectively, where

$$\begin{aligned} \mathcal{C}_0 &= \{p_{\Gamma_2}(\hat{\chi}) \leq p_2^* \wedge q = 0\}, \\ \mathcal{C}_1 &= \{p_{\Gamma_1}(\hat{\chi}) \geq p_1^* \wedge q = 1\}, \\ \mathcal{D}_0 &= \{p_{\Gamma_2}(\hat{\chi}) \geq p_2^* \wedge q = 0\}, \\ \mathcal{D}_1 &= \{p_{\Gamma_1}(\hat{\chi}) \leq p_1^* \wedge q = 1\}. \end{aligned} \quad (14)$$

This way, the angular velocity of the vehicle is  $\omega = qv(\gamma(\hat{\chi}) - \kappa\hat{e}_\theta) + (1 - q)\omega_{\text{user}}$ , where  $\omega_{\text{user}}$  is the angular velocity that the user imposes when he/she has the control authority.

#### IV. SIMULATIONS

The proposed controller has been extensively tested in simulations. In the results here reported, the controller parameters are set as follows:  $\kappa_x = 1$  and  $\kappa = 0.5$  in (10),  $p^* = p_1^* = p_2^* = 0.9$  in (14), and  $\Gamma_1 = -0.03$  and  $\Gamma_2 = -0.24$  for the thresholds of Definition 1. Since  $\Gamma_1$  and  $\Gamma_2$  are compared with  $-\kappa\hat{e}_\theta^2$  in (14), the corresponding mean tolerated attitude errors are  $15^\circ$  and  $40^\circ$ , respectively. The implemented localisation algorithm computing (4) is an extended Kalman filter fusing the odometric data with the absolute position measure from the landmarks [7]. The landmarks are deployed following [18] to ensure that at least one marker is always in the field of view of the camera (depicted with squares in Figure 5). The landmark reading uncertainty is  $10^\circ$  for the vehicle orientation and 10 cm for the position. The uncertainty due to encoders is of 13 mm per wheel revolute.

Recall that the underlying assumption of the proposed solution is that the path following performance of the proposed solution depends on the ability of the user to follow the path when the uncertainty grows. In fact, if the user is cooperative, rely on her/him is quite rewarding, while if the user is completely uncooperative (i.e. he/she constantly moves away from the path on purpose), the path following error grows. Notably, the user behaviour cannot be known in advance (and also, it is a challenging problem to define a suitable “cooperativeness” measure). Nevertheless when the path following error grows, the controller reliability as per Definition 1 grows as well, thus limiting the deviation from the planned path. In the simulations, when the user has the control authority, he/she is modelled with a neutral behaviour, that is he/she pushes the vehicle forward (i.e.  $\omega_{\text{user}} = 0$ ). Figure 5 shows the paths followed by the robot varying the landmark reading time  $\Delta t$ . Notice that if  $\Delta t$  is small (0, that is continuous reading, or 1 second) the vehicle is maintained close to the path, which is a trivial consequence of the small covariance (4) due to frequent landmarks readings: as a consequence, the robot remains in control most of the time. If  $\Delta t$  is larger (3 or 4 seconds), the controller reliability is, on average, smaller. In other words, the control authority is given to the robot only when the reliability exceeds the threshold  $p^*$ , which happens for larger mean values of  $\dot{V}$  (i.e. for larger attitude errors  $|e_\theta|$ , see (12)). Further simulations are presented in Figure 6, where the influence of landmark reading time  $\Delta t$  on the norm of the orientation error is shown in a probabilistic sense. For each  $\Delta t$ , 100 simulations are executed. Notice that, the larger  $\Delta t$ , the larger the attitude error  $e_\theta$ , since the user is endowed with more control authority in the presence of large uncertainty. A similar behaviour is obtained for the worst case distance to the path (see Figure 6, bottom plot).

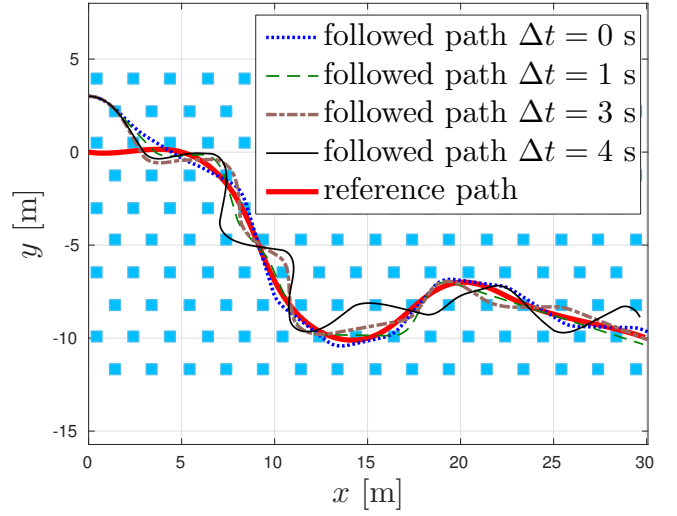


Fig. 5. Paths followed for different reading periods  $\Delta t$ . The squares represent the landmark positions.

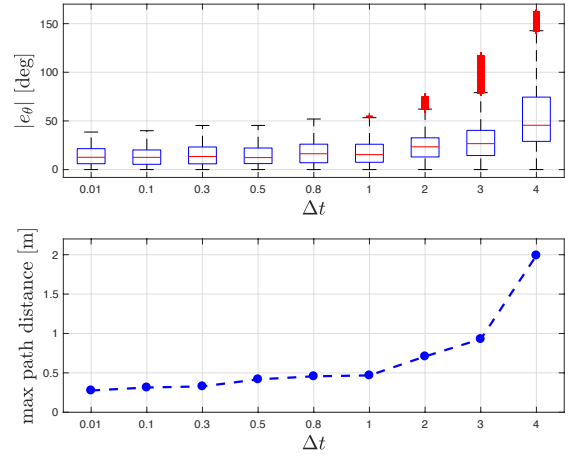


Fig. 6. Box and whiskers plot of  $|e_\theta|$  (top) and maximum path following error (bottom) for Montecarlo simulations with growing reading periods.

#### V. EXPERIMENTS

The experimental results have been collected using the *FriWalk* (Figure 1). The controller parameters adopted in the experiments are:  $\kappa_x = 1$ ,  $\kappa = 0.5$ ,  $p_1^* = 0.7$ ,  $p_2^* = 0.9$ ,  $\Gamma_1 = -0.004$  and  $\Gamma_2 = -0.137$ . With respect to the simulation results in Section IV, the probability  $p_1^*$  has been reduced to give more authority to the controller, thus increasing the user’s comfort. Similarly, both the mean tolerant attitude errors  $\Gamma_1$  and  $\Gamma_2$  have been reduced to  $5^\circ$  and  $30^\circ$ , respectively.

The experimental scenario is the Dept. of Information Engineering and Computer Science of the university of Trento, comprising corridors and rooms Figure 7. The starting point, of the *FriWalk* is inside one room, represented with a blue circle in Figure 7. Following the idea reported in Section I, the landmarks are placed only in proximity of difficult decision points, i.e. landmark #1 is in the starting room in the vicinity of the exit door, landmark #2 has been collocated at



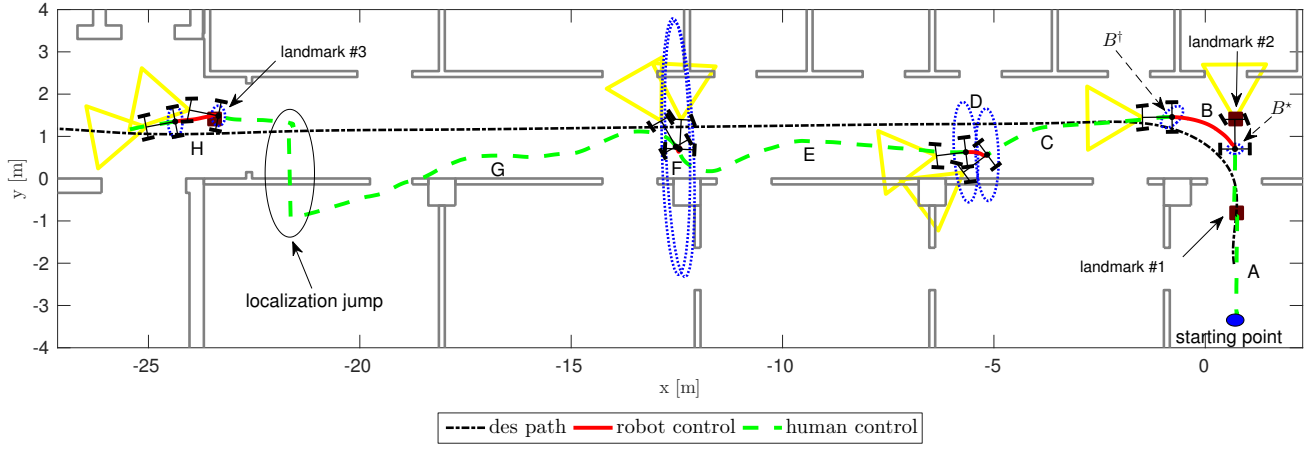


Fig. 7. A sample trajectory of the experimental trial with localization covariance depicted in selected points. The picture reports the desired path (dash-dotted line) and the estimated trajectory obtained by the localization algorithm (dashed line). This trajectory is divided into sub-paths for reading easiness.

the beginning of the corridor, while landmark #3 is deployed before two intersecting corridors. In the corridor, due to the particular desired path considered (dash-dotted black line of Figure 7), has no landmark since the only available choice is to maintain on the course. The depicted yellow solid triangle pointing forward represents the field of view of the camera attached to the vehicle and used to detect the landmarks, while the dotted blue ellipses represent the localisation error covariance  $P_{xy}$  (upper  $2 \times 2$  matrix of (4)) in selected positions. To better analyse the experiments, the path is divided in the following parts:

**Sub-path A:** the user is in control of the robot ( $q = 0$  in (13)) and pushes the *FriWalk* outside from the room since the localisation error is very high (i.e. kidnapped robot problem, dashed green line in Figure 7).

**Sub-path B:** when the vehicle detects a landmark in position  $B^*$ ,  $p_{\Gamma_2}(\hat{\chi}) > p_2^*$  and the controller (14) enters in the jump set  $\mathcal{D}_1$  so that  $q \rightarrow 1$ . The robot is hence in control ( $q = 1$  in Figure 4). The Gaussian probability density function (pdf) of  $\dot{V}$  in point  $B^*$  is reported with dash-dotted black line in Figure 8. During the *robot in control* state  $\omega$  is imposed by the control law and steers the walker toward the desired path (red solid line in Figure 7). At point  $B^\dagger$ ,  $p_{\Gamma_1}(\hat{\chi}) < p_1^*$  and the authority is given back to the user since  $q \rightarrow 0$  (the solid green Gaussian pdf in Figure 8).

**Sub-path C:** in this section the user is in control and the covariance  $P_{xy}$  grows (no landmark detected), hence the pdf flattens, so that it is more difficult for the controller to kick in. Nonetheless, at the end of sub-path C, the orientation error becomes so large (indeed,  $\dot{V}$  is a quadratic function of  $\hat{e}_\theta$  (10)) that  $p_{\Gamma_2}(\hat{\chi}) \geq p_2^*$  and the controller intervenes to align the user toward the path.

**Sub-path D:** due to the shape of the Gaussian, which is more flat than in sub-path B, it takes a smaller time to reach the condition  $p_{\Gamma_1}(\hat{\chi}) < p_1^*$ . However, the user receives the input to realign towards the desired path.

**Sub-path E:** the user has the possibility to move freely since the covariance of the localisation error is very high. At the

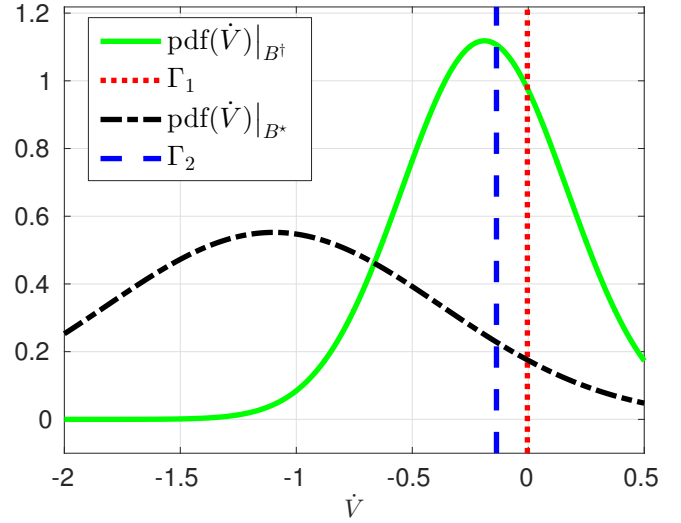


Fig. 8. Distribution of  $\dot{V}$  at the beginning of section  $B \rightarrow B^*$  (dash-dotted black line) and at the end of section  $B \rightarrow B^\dagger$  (solid green line).

end of this sub-path the user tried to perform an U-turn, but the controller do not allow this manoeuvre as at the end of Sub-path C.

**Sub-path F:** the same of sub-path D, but even shorter.

**Sub-path G:** from the beginning of this sub-path, no landmark is in view for 12.5 meters, so that the uncertainty grows unbounded. Notice that the walker wrongly localises through a wall, which is obviously not true: however, if the *robot in control* was active, the vehicle would be guided over the desired path and hence, aligning the green dashed line over the dash-dotted desired path, the *FriWalk* would be steered towards the wall on the other side of the corridor. Instead, after landmark #3 is detected and the uncertainty drops, it can be seen that the vehicle was correctly very close to the path, guided by the user.

**Sub-path H:** finally, the controller takes the control of the robot since  $p_{\Gamma_2}(\hat{\chi}) \geq p_2^*$ .

## VI. CONCLUSIONS

In this paper, we have presented a control strategy for shifting control authority between a human user and a controller for robotic navigation assistance. In this context, the problem of assisting a person can be seen as an instance of path following problems, for which most of the available solutions currently require an accurate localisation of the vehicle in the environment. This requirement comes along with the need for deploying a heavy infrastructure of landmarks in the environment, which is not always feasible in such spaces as museums or large shopping malls. Our idea to solve the problem is to use a precise localisation only when needed (i.e., in proximity of complex decision points) and leave the guidance responsibility to the user when the task is relatively easy to do (i.e., just keep going along a direction). This strategy requires an effective way to shift the control authority to the user when the localisation precision is low, and give it back to the controller when it increases (i.e., when more landmarks are in sight) or when the user is compromising the control goals (i.e., turning backwards). This idea has been formalised with a hybrid control design. The paper sets up the theoretical framework for this controller and shows its efficacy through extensive simulations and experimental results.

There are several open problems that deserve future investigation. From the theoretical point of view, the most interesting problem that needs to be addressed is to offer “certifiable” performance guarantees based on the knowledge of the vehicle and the environment. Another important goal is to test the idea with a number of actual users and carry out a quantitative and qualitative study on their performance and impressions.

## REFERENCES

- [1] U. Cortes, C. Barrue, A. B. Martinez, C. Urdiales, F. Campana, R. Annicchiarico, and C. Caltagirone, “Assistive technologies for the new generation of senior citizens: the share-it approach,” *International Journal of Computers in Healthcare*, vol. 1, no. 1, pp. 35–65, 2010.
- [2] M. Andreetto, S. Divan, D. Fontanelli, and L. Palopoli, “Path Following with Authority Sharing between Humans and Passive Robotic Walkers Equipped with Low-Cost Actuators,” *IEEE Robotics and Automation Letters*, vol. 2, no. 4, pp. 2271–2278, Oct. 2017.
- [3] L. Hedley, N. Suckley, L. Robinson, and P. Dawson, “Staying steady: a community-based exercise initiative for falls prevention,” *Physiotherapy theory and practice*, vol. 26, no. 7, pp. 425–438, 2010.
- [4] K.-T. Khaw, N. Wareham, S. Bingham, A. Welch, R. Luben, and N. Day, “Combined impact of health behaviours and mortality in men and women: The epic-norfolk prospective population study,” *PLoS Med*, vol. 5, no. 1, p. e12, 01 2008.
- [5] “ACANTO: A Cyberphysical social NeTwOrk using robot friends,” <http://www.ict-acanto.eu/acanto/>, February 2015, EU Project.
- [6] A. Colombo, D. Fontanelli, A. Legay, L. Palopoli, and S. Sedwards, “Efficient customisable dynamic motion planning for assistive robots in complex human environments,” *Journal of Ambient Intelligence and Smart Environments*, vol. 7, no. 5, pp. 617–633, 2015.
- [7] P. Nazemzadeh, F. Moro, D. Fontanelli, D. Macii, and L. Palopoli, “Indoor Positioning of a Robotic Walking Assistant for Large Public Environments,” *IEEE Trans. on Instrumentation and Measurement*, vol. 64, no. 11, pp. 2965–2976, Nov 2015.
- [8] D. Fontanelli, D. Macii, P. Nazemzadeh, and L. Palopoli, “Collaborative Localization of Robotic Wheeled Walkers using Interlaced Extended Kalman Filters,” in *Proc. IEEE Int. Instrumentation and Measurement Technology Conference (I2MTC)*. Taipei, Taiwan: IEEE, May 2016, pp. 1–6, available online.
- [9] P. Bevilacqua, M. Frego, E. Bertolazzi, D. Fontanelli, L. Palopoli, and F. Biral, “Path Planning maximising Human Comfort for Assistive Robots,” in *IEEE Conference on Control Applications (CCA)*. Buenos Aires, Argentina: IEEE, Sept. 2016, pp. 1421–1427.
- [10] M. Andreetto, S. Divan, D. Fontanelli, and L. Palopoli, “Harnessing Steering Singularities in Passive Path Following for Robotic Walkers,” in *Proc. IEEE International Conference on Robotics and Automation (ICRA)*. Singapore: IEEE, May 2017, pp. 2426–2432.
- [11] M. Andreetto, S. Divan, D. Fontanelli, L. Palopoli, and F. Zenatti, “Path Following for Robotic Rollators via Simulated Passivity,” in *Proc. IEEE/RSJ International Conference on Intelligent Robots and System (IROS)*. Vancouver, Canada: IEEE/RSJ, Oct. 2017, to appear.
- [12] D. Fontanelli, A. Giannitrapani, L. Palopoli, and D. Prattichizzo, “A Passive Guidance System for a Robotic Walking Assistant using Brakes,” in *Proc. IEEE Int. Conf. on Decision and Control (CDC)*. Osaka, Japan: IEEE, 15–18 Dec. 2015, pp. 829–834.
- [13] J.-P. Laumond, *Robot motion planning and control. Lectures Notes in Control and Information Sciences* 229, 1998, vol. 3.
- [14] Y. Bar-Shalom, X. Li, X. Li, and T. Kirubarajan, *Estimation with applications to tracking and navigation*. Wiley-Interscience, 2001.
- [15] P. Nazemzadeh, D. Fontanelli, D. Macii, and L. Palopoli, “Indoor Positioning of Wheeled Devices for Ambient Assisted Living: a Case Study,” in *Proc. IEEE Int. Instrumentation and Measurement Technology Conference (I2MTC)*. Montevideo, Uruguay: IEEE, May 2014, pp. 1421–1426.
- [16] A. Cameron and H. Durrant-Whyte, “A bayesian approach to optimal sensor placement,” *The International Journal of Robotics Research*, vol. 9, no. 5, pp. 70–88, 1990.
- [17] M. Beinhofer, J. Müller, and W. Burgard, “Effective landmark placement for accurate and reliable mobile robot navigation,” *Robotics and Autonomous Systems*, vol. 61, no. 10, pp. 1060–1069, 2013.
- [18] P. Nazemzadeh, D. Fontanelli, and D. Macii, “Optimal Placement of Landmarks for Indoor Localization using Sensors with a Limited Range,” in *International Conference on Indoor Positioning and Indoor Navigation (IPIN)*. Madrid, Spain: IEEE, Oct. 2016, pp. 1–8.
- [19] F. Zenatti, D. Fontanelli, L. Palopoli, D. Macii, and P. Nazemzadeh, “Optimal Placement of Passive Sensors for Robot Localisation,” in *Proc. IEEE/RSJ International Conference on Intelligent Robots and System (IROS)*. Daejeon, South Korea: IEEE/RSJ, Oct. 2016, pp. 4586–4593.
- [20] D. B. Jourdan and N. Roy, “Optimal Sensor Placement for Agent Localization,” *ACM Trans. Sen. Netw.*, vol. 4, no. 3, pp. 13:1–13:40, June 2008.
- [21] S. Martinez and F. Bullo, “Optimal sensor placement and motion coordination for target tracking,” *Automatica*, vol. 42, no. 4, pp. 661–668, 2006.
- [22] D. Moreno-Salinas, A. M. Pascoal, and J. Aranda, “Optimal Sensor Placement for Multiple Target Positioning with Range-Only Measurements in Two-Dimensional Scenarios,” *Sensors*, vol. 13, no. 8, p. 10674, 2013.
- [23] S. Se, D. Lowe, and J. Little, “Mobile robot localization and mapping with uncertainty using scale-invariant visual landmarks,” *The international Journal of robotics Research*, vol. 21, no. 8, pp. 735–758, Aug. 2002.
- [24] K. Lingemann, A. Nüchter, J. Hertzberg, and H. Surmann, “High-speed laser localization for mobile robots,” *Robotics and Autonomous Systems*, vol. 51, no. 4, pp. 275–296, Jun. 2005.
- [25] B. Sinopoli, L. Schenato, M. Franceschetti, K. Poolla, M. I. Jordan, and S. S. Sastry, “Kalman filtering with intermittent observations,” *IEEE Transactions on Automatic Control*, vol. 49, no. 9, pp. 1453–1464, Sept 2004.
- [26] U. Lee, J. Jung, S. Shin, Y. Jeong, K. Park, D. H. Shim, and I. s. Kweon, “EureCar turbo: A self-driving car that can handle adverse weather conditions,” in *2016 IEEE/RSJ International Conference on Intelligent Robots and Systems (IROS)*, Oct 2016, pp. 2301–2306.
- [27] D. Soetanto, L. Lapierre, and A. Pascoal, “Adaptive, non-singular path-following control of dynamic wheeled robots,” in *IEEE Conf. on Decision and Control*, vol. 2. IEEE, 2003, pp. 1765–1770.
- [28] R. Goebel, R. G. Sanfelice, and A. R. Teel, *Hybrid Dynamical Systems: modeling, stability, and robustness*. Princeton University Press, 2012.
- [29] M. Krstic, I. Kanellakopoulos, and P. V. Kokotovic, *Nonlinear and adaptive control design*. Wiley, 1995.